

Intuitive Control of Humanoid Soft-Robotic Hand BCL-13

Jianshu Zhou, *Student Member, IEEE*, XiaoJiao Chen, *Student Member, IEEE*, Ukyoung Chang, Jia Pan, *Member, IEEE*, Wenping Wang, *Fellow, IEEE* and Zheng Wang*, *Senior Member, IEEE*.

Abstract—Traditionally, robotic hand grasping is realized by rigid robotic hands or grippers, which requires high-resolution sensor feedback and delicate control algorithm. Recently, soft robotics has emerged as an alternative approach to humanoid robotic hand design. But due to distinctive material, structure, actuation mechanism, limited degrees-of-freedom (DOF) of soft robots, their control raised new challenges. Most existing soft robot control strategies are based on the simple on/off signal, rather than intuitive, real-time control for dexterous grasping and manipulation tasks. In this paper, we present an intuitive grasping control for our proprietary 13-DOF humanoid soft robotic hand, BCL-13. This control approach allows all the 13 independent DOFs to be controlled continuously by intuitive human hand poses. Real-time human hand joint angles are captured by Leap Motion Controller. Then the human hand joint angle position is mapped into the robotic hand joint through our dedicated filter. Finally, the robotic hand joint actuation commands are regulated by the lower-level pressure controller. With passive compliance, the proposed intuitive grasping process can achieve excellent grasping performance and safety without strict accuracy requirements. This approach shows potential for dexterous humanoid robotic hand control for safe and intuitive interactions.

Index Terms- Humanoid grasping and manipulation, Soft Robotics, End Effectors.

I. INTRODUCTION

Robotic hand is the interface between a robot and the surrounding environment and humans [1-3]. Traditional robotic hands usually have fingers connected by rigid pin joints, mostly driven by electric motors. They need high-resolution force and position sensor feedback, as well as delicate control algorithm to realize successful grasping and manipulation [4, 5]. The whole system requires high accuracy for both mechanism and control [6, 7]. Recently, soft robotics has emerged as a promising approach for humanoid robotic hand design [8-10]. Inherent compliance and adaptability of soft robotics make them suitable for safe human-robot interaction (e.g. service robots, rehabilitation robots, personal robots, etc.). Due to intrinsic compliance, soft grippers exhibit excellent adaptability to the unstructured environment [11-16]. This adaptability significantly reduces the complexity of the grasping system by getting rid of high accuracy sensory feedback and controller sophistications. Such benefits dramatically increase design flexibility and affordability of the robotic end-effector design.

The performance of soft robotic hand depends on the cooperation of the mechanism and control system. However,

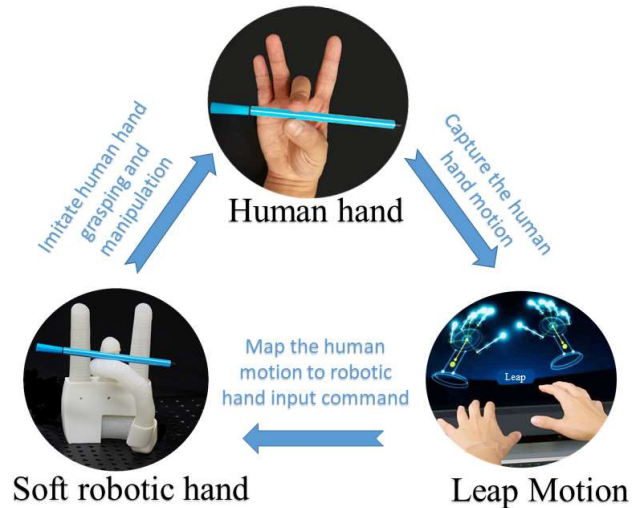


Figure 1. The concept of the proposed intuitive grasping control for the BCL-13 humanoid soft robotic hand.

the control strategies for existing soft robotic hands are mainly binary due to the solenoid valves, which are sufficient for existing soft robotic hands with low-DOF (typically 2-5) mechanisms [17-20]. Most soft robotic fingers are composed of one DOF pneumatic-driven soft actuator [17, 19, 20], trajectory of which follows a predefined curve and accept only one input reference.

A refined control strategy suitable for dexterous soft robotic hands with more DOFs will be helpful to enhance the grasping performance. In hand mechanism level, our previous work presented a dexterous humanoid soft robotic hand, BCL-13 [13], which has 13 fully actuated DOFs based on human hand model reduction. The mechanism of the hand is capable of dexterous grasping and in-hand manipulation [13]. Although the preliminary pressure based control presented in our previous work was effective for individual joint motion control, the challenges of the coordinative high-level control and action planning were not addressed due to the hand's significant dexterity combined with the inherent compliance of the target soft-robotic system [13].

In this paper, we propose an intuitive grasping control approach for humanoid soft robotic hand as illustrated in Fig. 1. This approach is based on the reduced joint-to-joint mapping, which maps the human hand joint motion onto the existing soft robotic hand joint [21-22]. Two characteristics of

Research jointly supported by Hong Kong RGC Grant 27210315, ITF Grant ITS/4571/17FP, ITS/140/18, HKU Seed Grant 201511159051, 201611159196, 201611160034, 201711160023, and 201711159158.

J. Zhou, X. Chen, U. Chang and Z. Wang are with the Department of Mechanical Engineering, The University of Hong Kong, Pokfulam, Hong Kong, SAR (e-mail: zhoujs@hku.hk; chen2014@hku.hk; ukchang@hku.hk; zwangski@hku.hk).

J. Pan is with the Department of Mechanical and Biomedical Engineering, City University of Hong Kong, Hong Kong (panjia1983@gmail.com).

W. Wang is with Department of Computer Science, The University of Hong Kong, Kowloon, Hong Kong (e-mail: wenping@cs.hku.hk).

J. Zhou and X. Chen are joint first authors.

*corresponding author, e-mail: zwangski@hku.hk, Tel: +852-3917-7905, Fax: +852-2858-5415.

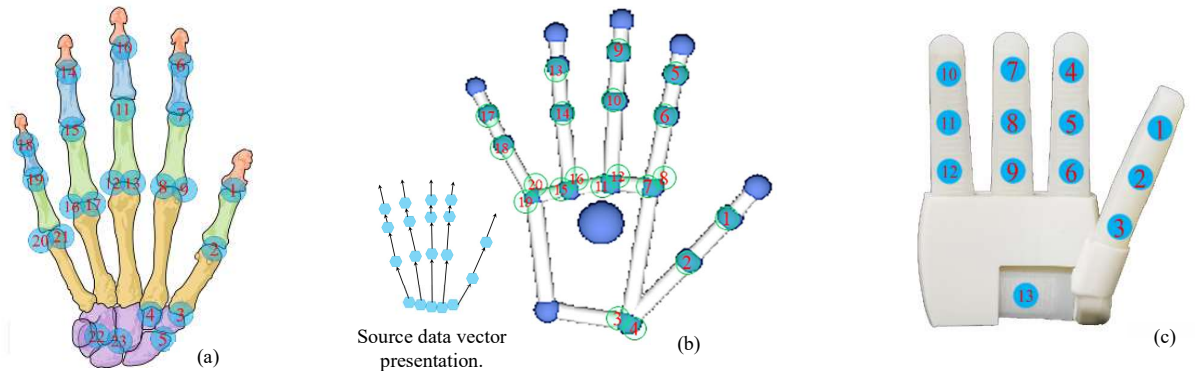


Figure 2. The hand kinematic models comparison. (a) A standard human hand model with 23 DOFs numbered H-1 to H-23. (b) The Leap-Motion-captured source data depicted as a 20-DOF model with DOFs numbered as L-1 to L-20. (c) The 13-DOF soft robotic hand model numbered as B-1 to B-13.

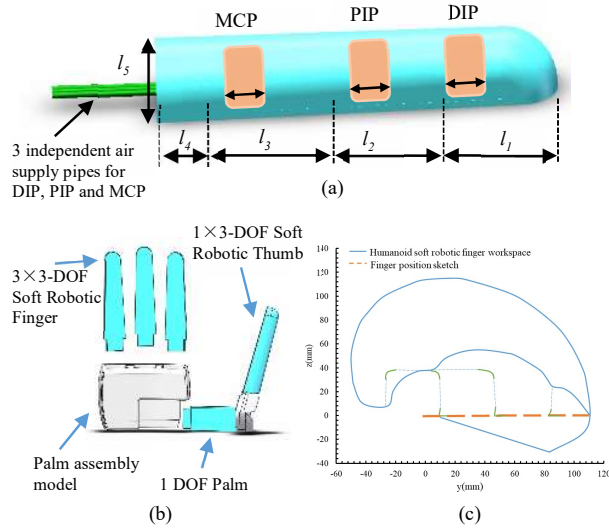


Figure 3. The BCL-13 humanoid hand. (a) The mechanism of 3 DOF humanoid soft robotic finger. (b) The assembly of BCL-13. (c) The humanoid robotic finger's workspace

soft robotic hands enable the reduced joint-to-joint mapping. One is the inherent compliance of the soft hands which compensates for the position inaccuracy caused by the hand model reduction. The second is the design intention for such soft hands are more focused on adaptable grasping and safe human-robot interaction, which grants some leniency on in-hand manipulation. Thus the reduced joint-to-joint mapping can be applied to the soft robotic hands. We capture the human hand motion through Leap Motion Controller (LMC) [23-25], which is then processed into the hand joint angle information. The joint angle information is mapped onto the robotic hand input value, which is air pressure in this work. The input pressure is sent to each joint of the robotic hand based on the pressure based control. Finally, the soft robotic hand can be intuitively controlled by the human hand motion.

Details of the human hand model reduction and reduced Joint-to-Joint mapping are discussed in Section II. In Section III, experiments are conducted with BCL-13 to validate the performance of the reduced Joint-to-Joint mapping based intuitive control.

Table I. Reduced joint-to-joint mapping between three kinematic models.

Order	Model DOF	Human hand	Leap hand	BCL-13
1.		H-1	L-1	B-1
2.		H-2	L-2	B-2
3.		H-3	L-3	B-3
4.		H-4	L4	B-13
5.		H-5	-	-
6.		H-6	L5	B-4
7.		H-7	L-6	B-5
8.		H-8	L-7	B-6
9.		H-9	L-8	-
10.		H-10	L-9	B-7
11.		H-11	L-10	B-8
12.		H-12	L-11	B-9
13.		H-13	L-12	-
14.		H-14	L13	B-10
15.		H-15	L-14	B-11
16.		H-16	L-15	B-12
17.		H-17	L-16	-
18.		H-18	L-17	-
19.		H-19	L-18	-
20.		H-20	L-19	-
21.		H-21	L-20	-
22.		H-22	-	-
23.		H-23	-	-

II. INTUITIVE GRASPING CONTROL FOR MULTI-DOF HUMANOID SOFT HAND

A. BCL-13, a 13 DOF humanoid soft robotic hand.

The humanoid soft robotic hand, BCL-13, used in our grasping control is presented in Fig. 2 [13]. BCL-13 has 13 DOFs with 4 fingers (Fig. 3(b)). Each finger has 3 fully actuated joints. With 3 independently controlled joints, the finger of BCL-13 can reach a human finger's workspace [13] (Fig. 3(c)). One palm DOF is designed to enable the thumb to oppose towards the other fingers to form a common workspace. Our previous work demonstrates the BCL-13 is capable of dexterous grasping and in-hand manipulation [13].

B. Reduced joint-to-joint mapping.

The proposed grasping control is based on capturing the human hand motion with LMC, then mapping the information of human hand motion into robotic hand input commands. To realize such intuitive grasping control, we have to study and understand the kinematics of different hand models first. Then we map the related joints across different models.

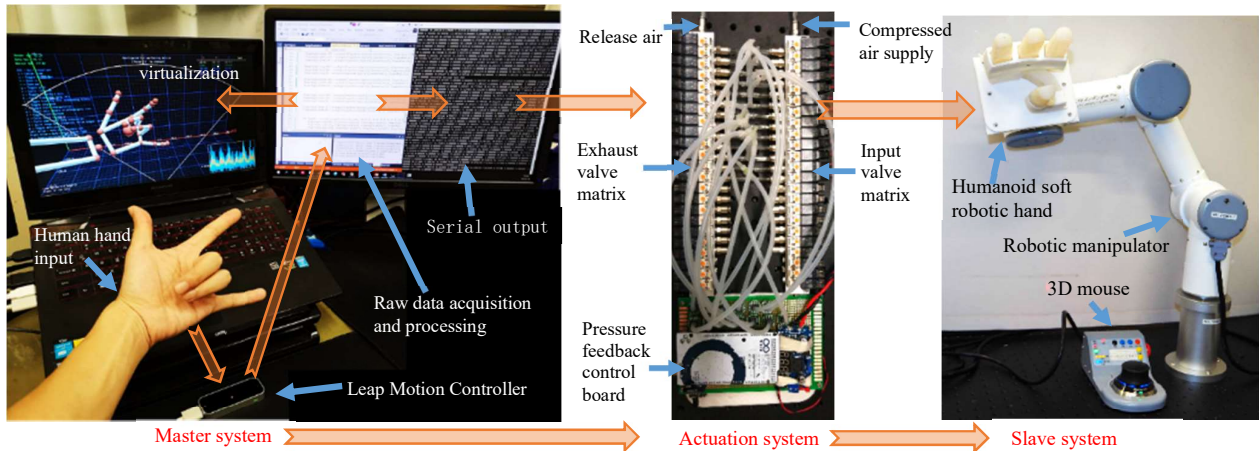


Figure 5. Intuitive grasping control system presentation. The master system is the Leap Motion Controller tracking the human hand pose. The acquisition data is processed by the software and then transmitted to the actuation system. The slave system, soft robotic hand, is actuated by the actuation system following the human hand pose.

There are three important hand kinematic models in this control: the human hand model, the Leap virtual hand model, and the humanoid soft robotic hand model, BCL-13.

The kinematic model of the human hand is illustrated by listing all the functional degree of freedoms (DOFs) in the hand. A commonly accepted 23-DOF human hand model is shown in Fig. 2(a) [26, 27], with 5 DOFs in the thumb, and 4 DOFs in each of four fingers, and the remaining 2 DOFs in the palm at the base of ring and little finger respectively [13]. The source data captured by LMC is the relative positions of each bone in the human hand, which are represented as vectors in space. The source data can be represented as a 20-DOF standard Leap virtual hand model as shown in Fig. 2 (b). The output kinematic model of BCL-13 is presented in Fig. 2(c). The DOFs of each model are numbered as H-1 to H-23, L-1 to L-20, and B-1 to B-13 respectively.

The reduced joint-to-joint mapping for the three models is presented in Table I. The 23 DOF human hand model is mapped to the 20 DOF Leap hand model. Two palm DOFs, H-22 and H-23, and one thumb DOF, H-5, were reduced in this mapping. Then, the 20-DOF Leap hand model is mapped to the BCL-13. In this mapping, the BCL-13 captured 12 DOFs in the bending joints except for the reduced little finger. One thumb opposition DOF in the palm can enable the thumb opposability. As a result, the BCL-13 can mimic the human finger bending range and the pose of the human hand.

C. Control and actuation of a single soft robotic DOF.

As shown in our previous work [13], [28]–[31], each joint was processed by a pressure based controller (PBC) to tune the input and exhaust pressure. Saturation filter, which is an automatic over-actuation protection mechanism, was used for each joint so that the maximum input pressure can be restricted within the range of bearable pressure. The single joint control diagram is illustrated in Fig. 4, including a saturation filter, a controller (C1), two solenoid valves regulating the pressure, and a pressure sensor used to feedback the real-time pressure of joint. Figure 8 features the hardware components containing a valve matrix and a pressure feedback control board to provide the regulated pressure to each joint.

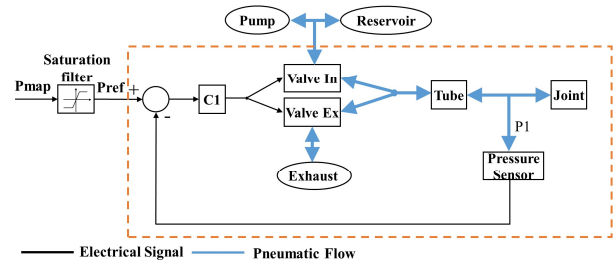


Figure 4. BCL-13 controller structure for a single joint. The dashed area presents the feedback control loop.

D. Intuitive grasping control system for soft robotic hand.

We present the intuitive grasping control system based on reduced joint-to-joint mapping for humanoid soft robotic hand. The whole system is illustrated in Fig. 5.

The master system is the LMC-based human hand tracking, with two monochromatic IR cameras and three infrared LEDs [21–23]. Human hand motion is the direct system input. The raw data of human hand information is captured and sent to the computer. The data is filtered through a dedicated filter. Then the processed data is transferred to the pressure based control and actuation system. The actuation system delivers the regulated pressure to each joint of robotic hand.

For small, light daily objects, successful grasping can be realized when soft fingers initiate a close contact with the targets. For relatively heavy objects, we set the fully curled human finger pose (i.e. a fist) as the robust grasping command, which enables the maximum pressure in the soft robotic fingers for grasping robustness. All joints of the robotic hand will exert the maximum output force in this condition.

In addition, a start command recognition was added to avoid sudden pose changes at the beginning of LMC capturing the human hand pose. The system will start after recognizing a thumbs-up gesture of human hand. Then the system will instruct you to release your hand and start grasping control. When more than one hands are recognized in the LMC detection region, the system will automatically stop and set all hand joints' pressure to zero.

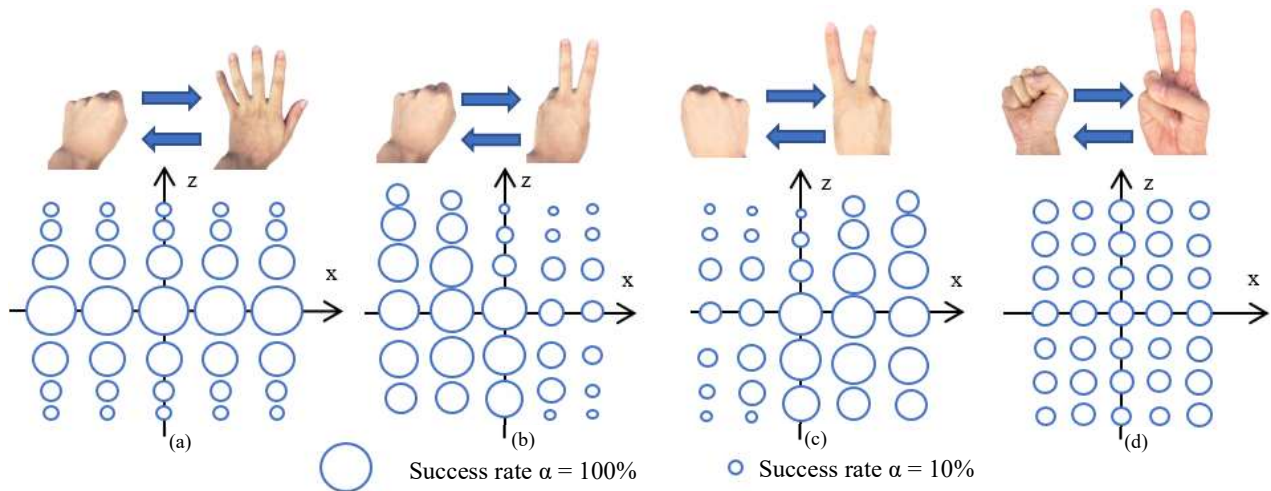


Figure 7. The success rate of different hand poses in different positions at a constant height. (a) Opening and closing of all five fingers of the left hand, with other digits closed and palm facing down. (b) Bending and stretching of the middle finger and index finger of the left hand, with other digits closed and palm facing down. (c) Bending and stretching of the middle finger and index finger of the right hand, with other digits closed and palm facing down. (d) Bending and stretching of the middle finger and index finger of the right hand, with other digits closed and palm facing up.

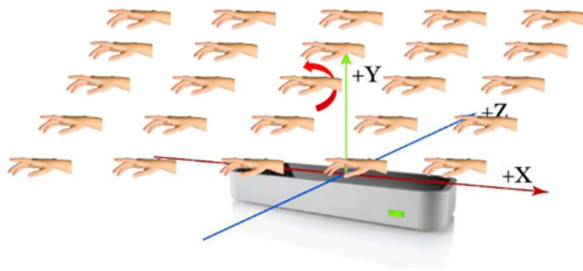


Figure 6. The experimental setup schematic.

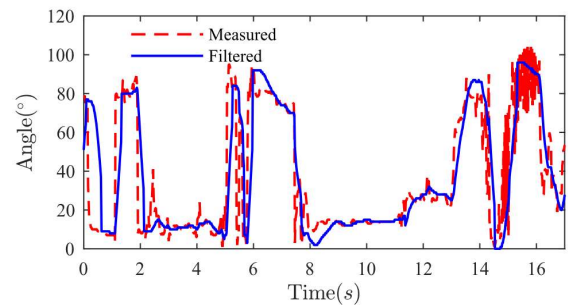


Figure 8. The data post-processing result.

III. GRASPING CONTROL REALIZATION AND PERFORMANCE

In this section, we present the realization and performance of our intuitive grasping control approach, which based on the reduced joint-to-joint mapping, for humanoid soft robotic hand.

A. Enhancement for the effectiveness of reduced joint to joint mapping.

At first we present our approach to enhance the effectiveness of joint-to-joint mapping. Two methods were adopted in our experiments. The first is to reduce the potential error in the input data by finding the proper hand pose and position. The second is to post-process the captured raw data attenuating the effect of undesired behavior caused by noise.

Although the LMC's tracking accuracy is excellent when stabilized, the dynamic tracking result is prone to error. To avoid this problem, most researchers extract gesture information from the raw data as an abstract layer and feed to their application. However, in our case, we try to directly track the angles in real-time, thus we should avoid the oscillations and errors, which may be caused during the data capturing. In order to identify the best location and angle for LMC recognition of the hand pose, we compared different hand poses at different points above the LMC at a constant height $h = 20\text{cm}$ to check the tracking performance, as shown in

Fig. 6. Each hand pose in a single testing point was tested for 20 times, and the number of successful tracking were recorded. The results of the success rate are represented by the relative circle size in Fig. 7.

In Fig. 7(a), the hand pose is to open and close all five fingers with the palm facing random direction. This is a commonly encountered situation for daily grasping. In our test, the success rate α was closely related to the normal distance of the hand to the x axis of the leap motion device. In Fig. 7(b), the hand pose is to open and close the index and middle finger of the left hand with all other digits closed and palm facing down. The results showed an uneven distribution, which favors the left side of the leap motion. On the contrary, with the right hand assuming the same pose, the higher success rate area is on the right (Fig. 7(c)). This can be explained by the detection principle of leap motion which relies on infrared light tracking. The index and middle fingers of the left hand would be subjected to a more reliable detecting on the left than on the right, where the hand itself would pose an obstruction. This is also demonstrated in Fig. 7(d). With the same hand pose but with the palm facing up, the success rate α is nowhere satisfactory. From this experiment, we can see that there is no fixed point for reliable measurement of the hand pose. The best solution to improving the success rate is exposing the relevant fingers directly on the leap motion platform without obstruction.

To obtain a smoother angle command, a Kalman filter of constant velocity model was used [32]. Assuming the process model has an acceleration following a normal distribution with mean $\mu = 0$, and variance σ^2 , as

$$\begin{bmatrix} x_{t+1} \\ \dot{x}_{t+1} \end{bmatrix} = \begin{bmatrix} 1 & dt \\ 0 & 1 \end{bmatrix} \begin{bmatrix} x_t \\ \dot{x}_t \end{bmatrix} + \begin{bmatrix} \frac{1}{2} dt^2 \\ dt \end{bmatrix} \ddot{x}_t. \quad (1)$$

And the model uncertainty could be written as

$$\begin{bmatrix} \frac{1}{2} dt^2 \\ dt \end{bmatrix} \ddot{x}_t \sim N(0, Q), \quad (2)$$

where

$$Q = \begin{bmatrix} \frac{1}{t} dt^4 & \frac{1}{2} dt^3 \\ \frac{1}{2} dt^3 & dt^2 \end{bmatrix} \sigma^2. \quad (3)$$

The measurement model is

$$z_t = [1 \ 0] \begin{bmatrix} x_t \\ \dot{x}_t \end{bmatrix} + v, \quad (4)$$

where $v \sim N(0, R)$. Different combinations of Q and R would result in different following manners. In this paper, we tried to negotiate between tracking accuracy and smoothing. Therefore, we chose an update rate $dt = 20ms$, $\sigma^2 = 100000$ and $R = 0.1$. The result of the middle finger MIP joint after implementing the Kalman filter is shown in Fig. 8. The filtered angle matched the measured data well and smoothed the oscillations to reduce the tremor of the robotic hand.

B. Intuitive grasping control performance.

In this section, we present the performance of the intuitive grasping control for humanoid soft robotic hand based on the reduced joint-to-joint mapping.

Three tests were conducted to present the grasping control. The first one is the individual finger motion control. The second test is the whole hand motion control. The third test is the grasping control of real objects.

The individual finger control performance is presented in Fig. 9(a-d). The 3-DOF humanoid fingers could mimic human finger bending better than 1-DOF counterparts in existing works, with the fingertip trajectory reaching a human-finger-like workspace. The success rate of individual finger control was 100% when the human hand was positioned in the best recognition area of LMC.

The whole hand grasping control performance is presented in Fig. 10. When the human hand poses a grasping gesture, the humanoid soft robotic hand will mimic the human hand motion to bend all fingers as shown in Fig. 10(a). We used a mango as an object for grasping. Fig. 10(b) presents a mango was sent to the grasping region of BCL-13. Fig. 10(c-d) present two kinds of successful grasping approaches toward the mango. The grasping dynamic process is presented in our attached video. The success rate of mango grasping was 100% when the human hand was positioned in the best recognition area of LMC.

The intuitive grasping control for daily objects was realized with a 6-axis manipulator. The manipulator in this study was controlled by a 3D mouse. We mounted the soft robotic hand on the end of the manipulator. The manipulator enabled the soft robotic hand to reach for the objects in the grasping range. The grasping targets were on the ground or handed by humans. The

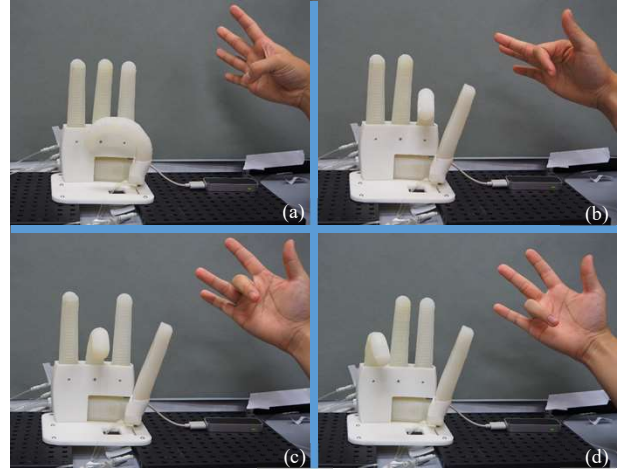


Figure 9. The finger motion tracking performance. (a) Thumb motion tracking. (b) Index finger motion tracking. (c) Middle finger motion tracking. (d) Ring finger motion tracking.

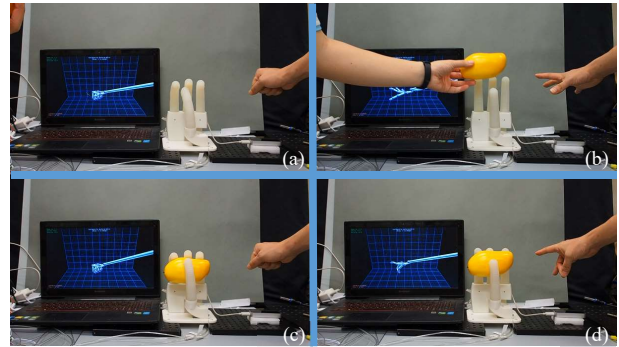


Figure 10. Real grasping performance on a mango. (a) Hand grasping condition. (b) Preparing for grasping. (c) Four fingers grasping a mango. (d) Two-finger pinch for a mango.

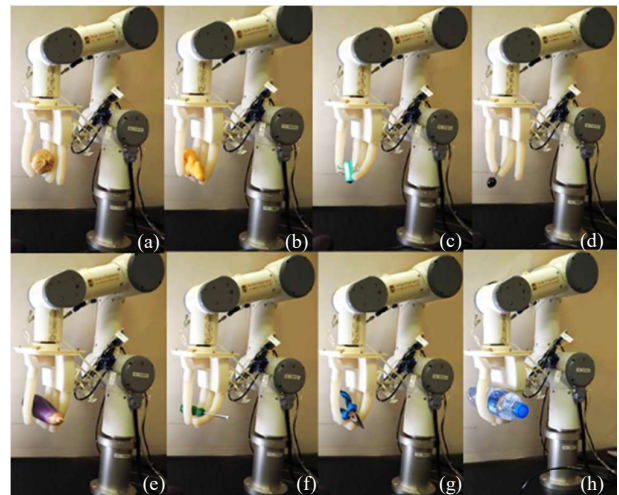


Figure 11. Daily object grasping with intuitive grasping control. (a) Garlic. (b) Ginger. (c) Metal Clasp. (d) Cherry. (e) Eggplant. (f) Screwdriver. (g) Pliers. (h) 700g Water bottle.

human hand above the LMC provided the grasping command to the BCL-13. For small, light objects, the BCL-13 can successfully grasp them when fingers form a closure region

around the objects (Fig. 11(a-d)). For heavier, larger objects, grasping can be realized by assuming the fist pose command (Fig. 11(e-h)). The robotic hand will be set to the maximum pressure in each joint for the maximum payload. Up to 700g water bottle can be firmly grasped by the soft robotic hand, as shown in Fig. 11(h). Under the maximum grasping force exertion, the hand will still maintain compliant interaction with the objects. Delicate objects like fruits and vegetables were undamaged under the maximum force grasping. With the intuitive grasping control, the soft robotic hand can provide suitable payload for daily objects and maintain inherent safety.

V. CONCLUSION AND FUTURE WORK

In this paper, we presented an intuitive grasping control approach for dexterous humanoid soft robotic hand, BCL-13. This approach is based on the reduced joint-to-joint mapping, which enables the 13-DOF humanoid soft robotic hand to replicate the human hand pose tracked by the Leap Motion Controller. We compared three different hand kinematic models, human hand model, Leap hand model, and the soft robotic hand model, for kinematic mapping towards grasping control. The whole system design and realization were illustrated in detail. Implementation of the intuitive grasping control on the BCL-13 hand was presented. For object grasping, soft robotic hand with inherent compliance could adapt to the shape of the grasping target by passively adjusting the contact area. With high dexterity of 13 DOFs, the humanoid hand can mimic the human hand to realize various hand functions. The grasping control performance of the soft robotic hand provides a promising approach for dexterous humanoid soft hands working in human-centered environments, requiring dexterous hand grasping function and safe human-robot interaction.

Future works include: refining the humanoid soft robotic hand to realize more dexterous human hand functions; adding real-time position feedback control for the soft robotic finger; combining the manipulator control with the intuitive grasping control, so that the complete grasping system could be controlled by the human hand poses. Thus, the robotic manipulator can follow the motion of human arm and the robotic hand can grasp the target; further investigations on soft robotic hand control and strategies for improving grasping adaptability and reliability.

REFERENCES

- [1] A. Bicchi and V. Kumar, "Robotic grasping and contact: A review," *Proceedings-IEEE Int. Conf. Robot. Autom.*, vol. 1, pp. 348–353, 2000.
- [2] M. R. Cutkosky, "On Grasp Choice, Grasp Models, and the Design of Hands for Manufacturing Tasks," *IEEE Trans. Robot. Autom.*, vol. 5, no. 3, pp. 269–279, 1989.
- [3] A. M. Dollar, A. Bicchi, M. R. Cutkosky, and R. D. Howe, "Special Issue on the Mechanics and Design of Robotic Hands," *Int. J. Rob. Res.*, vol. 33, no. 5, pp. 675–676, 2014.
- [4] Z. Wang, A. Peer, and M. Buss, "An HMM approach to realistic haptic Human-Robot interaction," *Proc. - 3rd Jt. EuroHaptics Conf. Symp. Haptic Interfaces Virtual Environ. Teleoperator Syst. World Haptics 2009*, pp. 374–379, 2009.
- [5] L. U. Odhner et al., "A compliant, underactuated hand for robust manipulation," *Int. J. Rob. Res.*, vol. 33, no. 5, pp. 736–752, 2014.
- [6] J. K. Salisbury and J. J. Craig, "Articulated Hands: Force Control and Kinematic Issues," *Int. J. Rob. Res.*, vol. 1, no. 1, pp. 4–17, 1982.
- [7] Zhou J, Yi J, Wang Z. A Rotational Tri-fingered Gripper for Stable Adaptable Grasping. 2018 IEEE International Conference on Real-time Computing and Robotics (IEEE RCAR 2018). 2018.
- [8] D. Rus and M. T. Tolley, "Design , fabrication and control of soft robots," 2015.
- [9] P. Polygerinos et al., "Towards a soft pneumatic glove for hand rehabilitation," *IEEE Int. Conf. Intell. Robot. Syst.*, pp. 1512–1517, 2013.
- [10] P. Polygerinos, Z. Wang, K. C. Galloway, R. J. Wood, and C. J. Walsh, "Soft robotic glove for combined assistance and at-home rehabilitation," *Rob. Auton. Syst.*, vol. 73, pp. 135–143, 2015.
- [11] Zhou J, Chen S, Wang Z. A Soft-Robotic Gripper With Enhanced Object Adaptation and Grasping Reliability. *IEEE Robotics and Automation Letters*, 2017, 2(4): 2287-2293.
- [12] Zhou J, Chen X, Li J, et al. A soft robotic approach to robust and dexterous grasping. *IEEE International Conference on Soft Robotics (RoboSoft)*. IEEE, 2018: 412-417.
- [13] Zhou J, Yi J, Chen X, et al. BCL-13: A 13-DOF Soft robotic hand for dexterous grasping and in-hand manipulation. *IEEE Robotics and Automation Letters*, 2018, 3(4): 3379-3386.
- [14] K. C. Galloway et al., "Soft Robotic Grippers for Biological Sampling on Deep Reefs," *Soft Robot.*, vol. 3, no. 1, pp. 23–33, 2016.
- [15] R. Deimel and O. Brock, "A compliant hand based on a novel pneumatic actuator," *Proc. - IEEE Int. Conf. Robot. Autom.*, pp. 2047–2053, 2013.
- [16] R. Deimel and O. Brock, "A novel type of compliant and underactuated robotic hand for dexterous grasping," *Int. J. Rob. Res.*, vol. 35, no. 1–3, pp. 161–185, 2016.
- [17] P. Polygerinos et al., "Modeling of Soft Fiber-Reinforced Bending Actuators," *IEEE Trans. Robot.*, vol. 31, no. 3, pp. 778–789, 2015.
- [18] P. Polygerinos et al., "Mosadegh B, Polygerinos P, Keplinger C, et al. Pneumatic Networks for Soft Robotics that Actuate Rapidly[J]. *Advanced Functional Materials*, 2014, 24(15):2109-2109."
- [19] Z. Wang, P. Polygerinos, J. T. B. Overvelde, K. C. Galloway, K. Bertoldi, and C. J. Walsh, "Interaction Forces of Soft Fiber Reinforced Bending Actuators," *IEEE/ASME Trans. Mechatronics*, vol. 22, no. 2, pp. 717–727, 2017.
- [20] A. D. Marchese, R. K. Katzschmann, and D. Rus, "A Recipe for Soft Fluidic Elastomer Robots," vol. 2, no. 1, pp. 7–25, 2015.
- [21] Ciocarlie M T, Allen P K. Hand posture subspaces for dexterous robotic grasping. *The International Journal of Robotics Research*, 2009, 28(7): 851-867.
- [22] Gioioso G, Salvietti G, Malvezzi M, et al. Mapping synergies from human to robotic hands with dissimilar kinematics: an approach in the object domain[J]. *IEEE Transactions on Robotics*, 2013, 29(4): 825-837.
- [23] H. Jin, Q. Chen, Z. Chen, Y. Hu, and J. Zhang, "Multi-LeapMotion sensor based demonstration for robotic refine tabletop object manipulation task," *CAAI Trans. Intell. Technol.*, vol. 1, no. 1, pp. 104–113, 2016.
- [24] D. Bassily, C. Georgoulas, J. Güttler, T. Linner, T. Bock, and T. U. München, "Intuitive and adaptive robotic arm manipulation using the leap motion controller," *Isr Robot.*, pp. 78–84, 2014.
- [25] G. Marin, F. Dominio, and P. Zanuttigh, "Hand gesture recognition with leap motion and kinect devices," 2014 IEEE Int. Conf. Image Process. ICIP 2014, pp. 1565–1569, 2014.
- [26] Sturman D J. Whole-hand input [D]. Massachusetts Institute of Technology, 1992.
- [27] I. A. Kapandji, *The physiology of the joints: Upper Limb*, vol. 1, 5th ed. New York: Elsevier, 1986.
- [28] P. Polygerinos, K. C. Galloway, E. Savage, M. Herman, K. O. Donnell, and C. J. Walsh, "Soft robotic glove for hand rehabilitation and task specific training," 2015 IEEE Int. Conf. Robot. Autom., vol. 2015–June, no. June, pp. 2913–2919, 2015.
- [29] X. Chen, S. Member, Z. Wang, and S. Member, "Soft-actuator-based Robotic Joint for Safe and Forceful Interaction with Controllable Impact Response," 2018.
- [30] X. Chen et al., "A Robotic Manipulator Design with Novel Soft Actuators," pp. 1878–1884, 2017.
- [31] J. Yi, X. Chen, C. Song, and Z. Wang, "Fiber-Reinforced Origami Robotic Actuator," *Soft Robot.*, vol. 00, no. 00, p. soro.2016.0079, 2017.
- [32] M. S. Arulampalam, S. Maskell, N. Gordon, and T. Clapp, "A tutorial on particle filters for online nonlinear/nongaussian bayesian tracking," *Bayesian Bounds Param. Estim. Nonlinear Filtering/Tracking*, vol. 50, no. 2, pp. 723–737, 2007.